Available online at BCREC website: https://bcrec.id

Bulletin of Chemical Reaction Engineering & Catalysis, 18 (4) 2023, 688-699

Research Article

Synthesis and Characterization of TiO_2-ZnO Nanocomposite Photocatalyst for the Removal of Basic Violet 14 as an Industrial Dye

Md. Abdullah Bin Samad[1,*], Emran Quayum[2], Md. Amjad Hossain[3], Tajmeri S.A. Islam[2], Mohammad Mahmudur Rahman Khan[1]

[1]*Department of Textile Engineering, Bangladesh University of Business and Technology (BUBT), Dhaka, Bangladesh.*
[2]*Department of Chemistry, University of Dhaka, Bangladesh.*
[3]*Institute of Leather Engineering and Technology, University of Dhaka, Bangladesh.*

Received: 19th October 2023; Revised: 26th November 2023; Accepted: 27th November 2023
Available online: 27th November 2023; Published regularly: December 2023

Abstract

Binary nanocomposites are one of the promising photocatalysts for the photodegradation of toxic industrial organic dyes which are used as dying agents in different industries including garments and textiles, leather, paint and varnish industries. For this study, TiO_2-ZnO nanocomposites were fabricated by the hydrothermal process; where $ZnSO_4.7H_2O$ is used as a precursor and TiO_2 is used as a supporting material. The prepared TiO_2-ZnO nanocomposites were calcined at three distinct temperatures 300 °C, 400 °C, and 500 °C. These composite materials were characterized by Scanning Electron Microscope (SEM), X-Ray Diffraction (XRD), Energy Dispersive X-Ray (EDX) analysis, and Fourier Transform Infrared (FTIR) spectroscopy. Basic Violet 14 (BV14), an industrial dye, was modelled to examine the photocatalytic role of TiO_2-ZnO under different experimental setups such as calcined temperatures, catalyst loading, concentrations of the BV14 dye, pH, and light sources. TiO_2-ZnO prepared at 500 °C acted as the best photocatalyst among three nanocomposites and the prepared TiO_2-ZnO worked better than solitary TiO_2 and ZnO to decolorize the BV14 dye. In the presence of sunlight, UV light, and visible light the percentages of degradation of BV14 were found to be 81.78 %, 69.58 %, and 31.24 %, respectively. The maximum photodegradation corresponded to 0.175 g/100 mL of suspension of nanocomposite with an initial 3.0×10^{-5} M of BV14 having solution pH 6.88. The surface reaction constant and Langmuir-Hinshelwood adsorption constant were obtained to be 5.5×10^{-8} mol.L^{-1}.min^{-1} and 1.7×10^{8} L.mol^{-1}, respectively.

Keywords: Industrial effluent; photodegradation; Basic Violet 14; photocatalyst; nanocomposite

How to Cite: M.A.B. Samad, E. Quayum, M.A. Hossain, T.S.A. Islam, M.M.R. Khan (2023). Synthesis and Characterization of TiO_2-ZnO Nanocomposite Photocatalyst for the Removal of Basic Violet 14 as an Industrial Dye. *Bulletin of Chemical Reaction Engineering & Catalysis*, 18(4), 688-699 (doi: 10.9767/bcrec.20059)

Permalink/DOI: https://doi.org/10.9767/bcrec.20059

1. Introduction

The disposal of different industrial effluents has grown into a significant issue in Bangladesh due to the country's recent fast industrial expansion [1]. Among several types of industries, readymade garments and leather industries use an enormous volume of water regularly and accordingly produce a vast quantity of liquid pollutants, which have a variety of toxic heavy metals and harmful organic and inorganic compounds [2]. These effluents are generally dumped without any prior treatment or with relatively minimal treatment to lakes and riv-

* Corresponding Author.
Email: samad@bubt.edu.bd (M.A.B. Samad)

ers. Textile sector, the largest water consumer, is dumping various types of synthetic dyes and textile effluents which are extremely hazardous and carcinogenic [3,4]. Several materials are used to treat these effluents and dyes.

Due to their delicate sizes with enormous specific surface areas, nanoscale composite materials typically exhibit remarkable electrical, optical, magnetic, and chemical properties that are markedly divergent from those of bulk materials. Pure ZnO powder has a higher photodegradation rate than that of pure TiO_2 and it follows the pseudo- first order kinetics [5,6]. It is possible to achieve a more effective charge separation, and an improved interfacial charge transfer to the adsorbed compounds conducing their photodegradation efficiency through joining two semiconductors with different energy levels for their corresponding conduction and valence bands [7]. To improve performance, various TiO_2-ZnO heterogeneous [8,9] composite photocatalysts of nanoparticles have been prepared and studies have been made to observe their effects, and the pseudo-first order kinetics is also observed [10,11]. ZnS-TiO_2 and ZnO-TiO_2, two binary composites of zinc and titanium compounds, were synthesized, characterized, and used as photocatalysts to degrade textile dyes [12–15]. The band gap of TiO_2-ZnO (3.09 eV) is lower than that of solitary TiO_2 (3.20 eV) and ZnO (3.29 eV). So, the photocatalytic performance of this composite photocatalyst (TiO_2-ZnO) is greater than that of these solitary metal oxides. Semiconducting powders made by the coupling of ZnO and TiO_2 exhibited photoactivities better than those of solitary TiO_2 and ZnO [16]. Nowadays, TiO_2-ZnO-mediated photodegradation of organic dyes is widely studied by many researchers [17–19]. Although composite TiO_2–ZnO and ZnO-supported natural volcanic Algerian clay (ZnO/CNA) showed better photocatalytic activity under solar light [20,21], a little research was done on comparison of photodegradations of organic dyes by using visible and UV light sources. It is true that synthesis, characterization and application of semiconductor photocatalysts, such as ZnO, TiO_2, and their nanocomposites, were investigated by many researchers around the world [22–29]. However, little information has been gleaned on the efficiency of those photocatalysts to degrade the dyes by the variation of different experimental conditions including various light sources, catalyst loading, pH, concentration of dye, and so on. Therefore, it is vividly clear that no study has been conducted before on the photodegradation of Basic Violet 14 (BV14) dye using nanocomposite TiO_2-ZnO mediated surface which strongly motivates the authors.

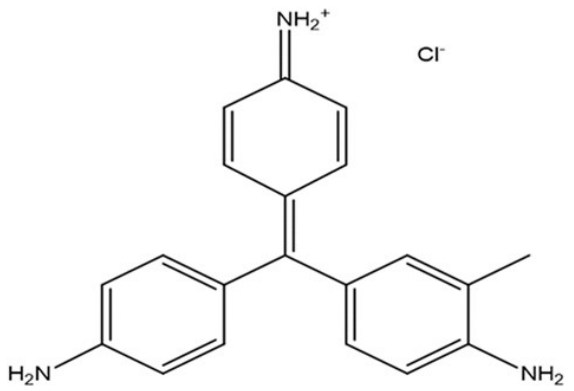

Figure 1. Chemical structure of Basic Violet 14 (BV14) dye.

In the present study TiO_2-ZnO nanocomposite photocatalysts have been synthesized and calcined at 300 °C, 400 °C, and 500 °C temperatures and then were characterized by the SEM, FTIR, XRD and EDX. Photodegradation of BV14 is explored to study their application by varying calcined temperatures, catalyst loading, solution pH, light sources and initial concentrations of BV14. The chemical structure of BV14 is given in the Figure 1.

2. Materials and Methods

2.1 Preparation of Nanocomposite

To prepare TiO_2-ZnO nanocomposite, $ZnCO_3$ was prepared in-situ from the aqueous solution of $ZnSO_4.7H_2O$ (Xilong Scientific Co., Ltd.) and $(NH_4)_2CO_3$. In this connection, solutions of $ZnSO_4.7H_2O$ and $(NH_4)_2CO_3$ (Merck, India) were prepared separately. $(NH_4)_2CO_3$ was slowly mixed with $ZnSO_4$ at the same time TiO_2 (Chemours Company, US) was mixed with uninterrupted stirring until a precipitation is formed. A medium heat was applied to speed up the reaction. The precipitation was divided into three parts. Then these three parts in three crucibles were heated individually in Muffle furnace (Isyzu Seisarysho Co., Ltd) for 4 h at 300 °C, 400 °C and 500 °C respectively. In the nanocomposites the ratio of TiO_2 and ZnO was 1:2. The nanocomposites prepared at 300 °C, 400 °C and 500 °C were denoted as A_1, A_2, and A_3. ZnO was synthesized from $ZnSO_4.7H_2O$ without adding TiO_2 [16,19]. The composite photocatalysts were characterized by Scanning Electron Microscope (SEM) (JSM-6490, JEOL, and Japan) and Energy Dispersive X-ray (EDX) (6490-LA, JEOL and Japan) to assess the surface morphology and confirm the pres-

ence of composition of the composites respectively. They were also investigated by X-ray Diffraction (XRD) (XRD-6100, Shimadzu and Japan) and Fourier Transform Infrared (FTIR) spectroscopy (SHIMADZU Prestige-21 and Japan) to apprise the phase composition and components of nanocomposite. Flowchart of a preparative method of the nanocomposite TiO_2-ZnO is given in the Figure 2.

2.2 Photodegradation Process

In a 100 mL glass beaker photodegradation of Basic Violet 14 (BV14) (Raj Chemicals, Gujarat, India) dye was investigated. Suspension of nanocomposite was prepared by taking a varying amount of nanocomposites in 20 mL of deionized water. Then this suspension was sonicated for 30 minutes by an ultrasonicator. Each suspension containing the BV14 dye solution of 3.0×10^{-5} M was irradiated under UV light and the change in BV14 concentration was measured at specific time intervals using the spectrophotometer. The photodegradation was carried out for 2 h. To investigate the effect of calcination temperature, nanocomposites are prepared at three different calcined temperatures and these nanocomposite suspensions (0.10 g/100 mL) containing 3.0×10^{-5} M concentration of BV14 are irradiated under UV light for 2 h. As photocatalytic efficiency of A_3 nanocomposite was maximum, the rest of the investigations was done by differing the amount of A_3 nanocomposite in the suspension. The effect of the BV14 concentration was observed from 3.0×10^{-5} M to 4.5×10^{-5} M on its photodecomposition with 0.175 g/100 mL suspension for 2 h under UV light. The pH effect on the photodegradation was also investigated for this experimental condition. Initial pH was balanced with dilute HNO_3 (Merck, India) and dilute NaOH (Merck, India) solutions. The NaOH solution was added very carefully to avoid extra crowding in the medium. In this case the concentration of BV14 and A_3 nanocomposite suspension were 3.0×10^{-5} M and 0.175 g/100 mL, respectively. The effect of UV, visible and sunlight was assessed on degradation of BV14. The wavelength used in the UV-visible spectrophotometer (UV-1800PC, Shimadzu, Japan) was 254 nm. An intense peak at 543 nm was observed in the spectrum. This peak has been taken as the working λ_{max} to follow the concentration of BV14.

3. Results and Discussion

3.1 Characterization of Prepared TiO_2-ZnO Composite

Figure 3 shows the SEM images of prepared composite A_1, A_2, and A_3. The particle sizes were 83 nm and 97 nm for nanocomposite A_1 and A_2 respectively (both are spherical) in shape and nanocomposite A_3 has particles with rod-like shape. Differentiation between TiO_2 and ZnO in the nanocomposite cannot be ob-

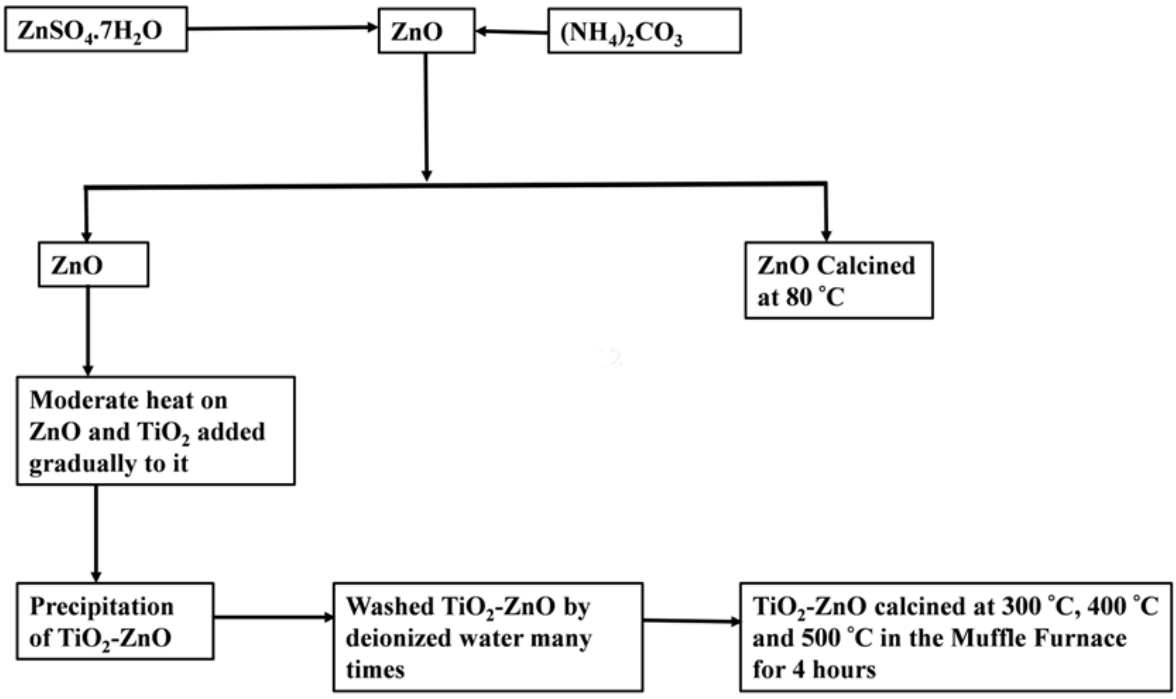

Figure 2. Flowchart for the preparation of TiO_2-ZnO nanocomposites.

tained from SEM images due to the similar electronic arrangement of Ti and Zn [19]. That is why the prepared nanocomposites need to be characterized by the patterns of XRD to observe the better understanding of the crystal lattices. EDX spectra of the prepared A_3 nanocomposite are shown in the Figure 4. The spectra show the peaks for Ti, Zn, and O only which indicate the purity of the composite. The ZAF standardless method was used to know the abundance of zinc, titanium, and oxygen elements in the sample. From the standardless quantitative analysis, it was found that the ratio of Ti, Zn, and O is 1: 5.7:5.1 in the prepared nanocomposite. An initial ratio of Ti, Zn, and O was 1:2:4. This finding demonstrates that ZnO and TiO_2 interacted at the molecular level in the nanocomposite, demonstrating that the prepared sample is a nanocomposite of ZnO and TiO_2 and not just a mechanical mixture of ZnO and TiO_2 [30]. Figure 5 displays the comparative FTIR spectra of prepared A_3 nanocomposite with ZnO and commercial TiO_2. Infrared spectra obtained from FTIR were recorded in solid phase using the KBr pellets in the range of wavenumber 4000–450 cm^{-1}. The broad band features below 1200 cm^{-1} are the result of overlapping Ti–O and Zn–O modes [31,32]. The bands 659.04 cm^{-1} and 999.0 cm^{-1} are assigned to the stretching vibration mode of Zn–O and Ti–O bonds, respectively. The vibration peak at about 1200 cm^{-1} is assigned to the FTIR spectra of pure TiO_2 [33]. The observed broad bands of absorption at around 300 cm^{-1} and 3500 cm^{-1} in ZnO and TiO_2 are attributed to the presence of moisture, which are abolished from the spectrum of nanocomposite. The comparative XRD patterns of prepared nanocompo-

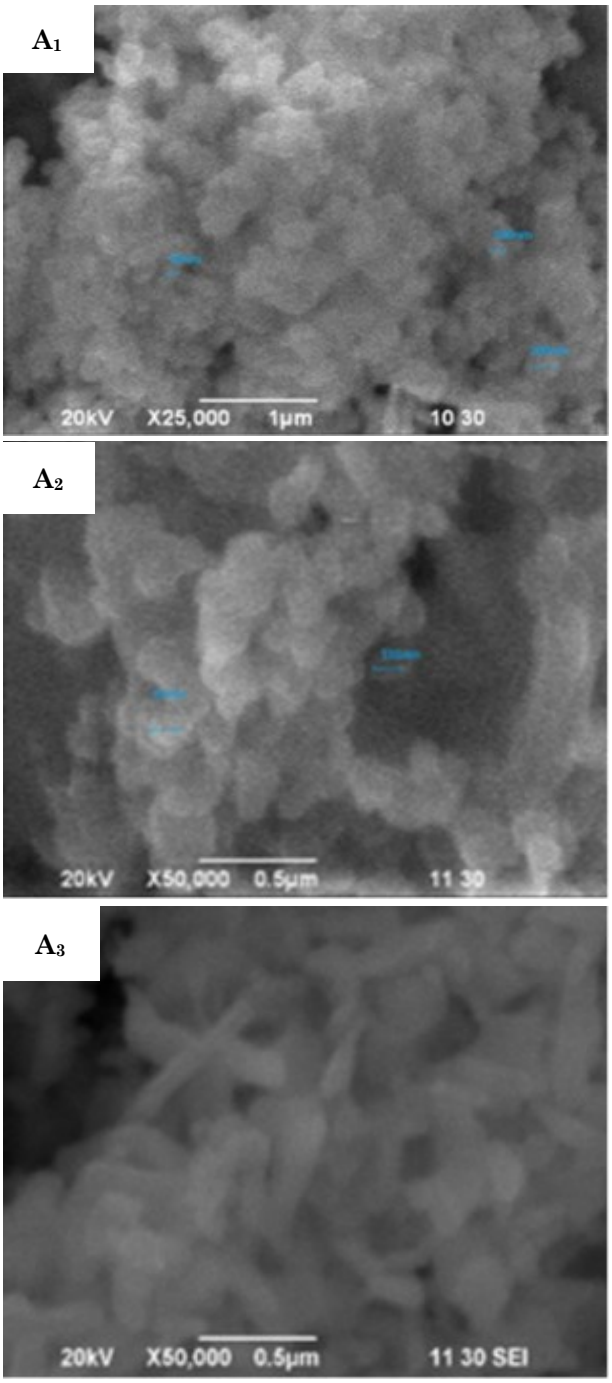

Figure 3. SEM images of composites.

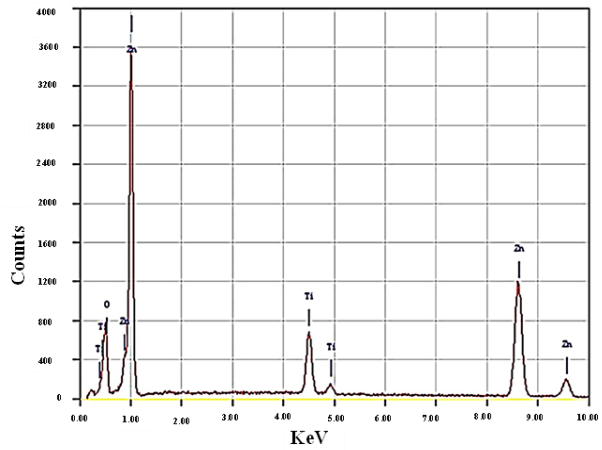

Figure 4. EDX spectra of TiO_2-ZnO composite.

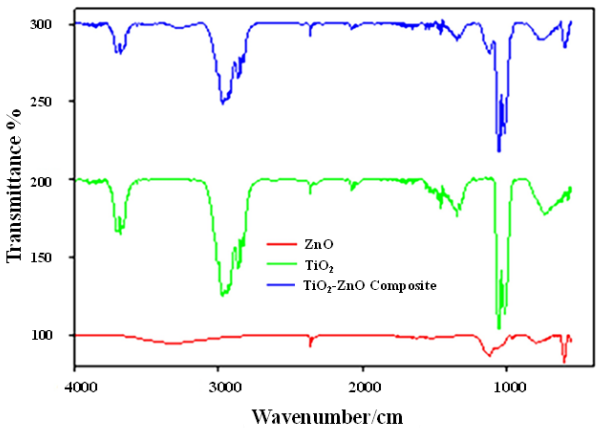

Figure 5. Transmittance vs. Wavenumber.

site TiO_2-ZnO with ZnO and commercial TiO_2 were shown in the Figure 6. All the diffraction peaks can be indexed to the hexagonal phase ZnO reported in JCPDS card (No. 36-1451, a = 0.3249 nm and c = 0.5206 nm). Four peaks appear at 31.77°, 34.42°, 36.25°, and 47.50° which correspond to (100), (002), (101), and (102), respectively [34]. It is clear from this observation that the prepared sample is ZnO. The XRD patterns of commercial TiO_2 show five peaks at 25.7°, 37°, 38°, 39°, and 48° which correspond to (101), (103), (004), (112), and (200), respectively. All these diffraction peaks can be indexed to the anatase phase TiO_2 reported in JCPDS card (No. 84-1286) [19,35]. The XRD patterns of prepared composite contain the diffraction peaks of ZnO at 31.77° and 47.50°. It also contains the diffraction peaks of anatase TiO_2 at 25.7°, 38°, and 39°. However, the (101) plane of ZnO and (103) and (200) planes of anatase TiO_2 are missing in the XRD patterns of the prepared nanocomposite. It suggests that TiO_2 and ZnO interacted at the molecular level, and the synthesized sample is most likely a nanocomposite photocatalyst of TiO_2 and ZnO [19].

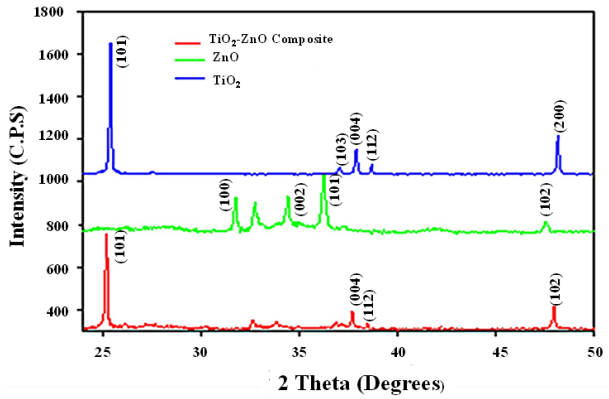

Figure 6. XRD patterns comparison.

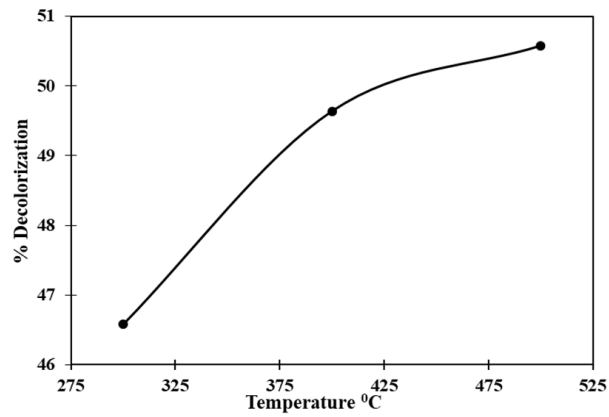

Figure 7. Temperature variation curve.

3.2 Effects of Calcined Temperature on the Photodegradation

With the rise of calcined temperature of prepared nanocomposite, percentage degradation gradually increases as shown in the Figure 7. The photodegradations of BV14 using A_1, A_2 and A_3 nanocomposite were 46.58%, 49.64%, and 50.58%, respectively. When the calcined temperature was 500 °C, the shape of the particles in composites changed from spherical to rod-like. The surface area of the composite having rod-like shape increases so adsorption also increases. This can be attributed to the fact that the enhancement of photodegradation of BV14 was the highest in A_3 composite [19].

3.3 Effects of Catalyst Loading

Finding out optimal loading of the catalyst is an efficient way to decolorize the dye molecules. A series of investigations were done by altering the amount of photocatalyst from 0.05 g/100 mL to 0.20 g/100 mL and keeping the concentration of BV14 constant at 3.0×10^{-5} M. Figure 8 shows that photodegradation of BV14 initially increases with the increase of concentration of nanocomposite, passes through a maxima and then decreases. The maxima correspond to the value of 0.175 g/100 mL of suspension. The total surface area enhances with enhancing nanocomposite dose, at the same time increasing in the turbidity of the suspension results a decrease in UV light penetration [36] because of increased scattering effect and hence photoactive volume of suspension decreases [37]. Furthermore, it is difficult to maintain the suspension homogeneous due to particle agglomeration at higher catalyst loading, and this causes a decreasing number of active sites which bring on lower photodegrada-

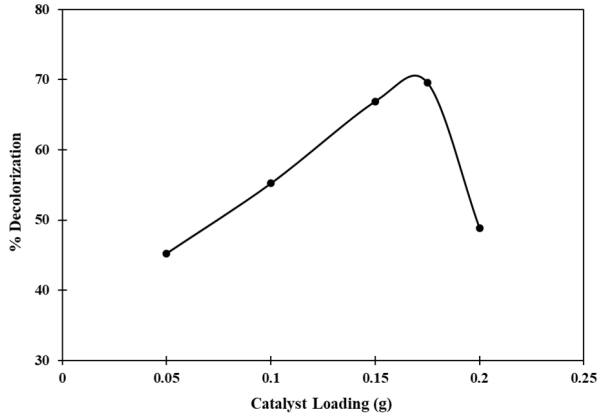

Figure 8. The effect of catalyst loading on the photodegradation of BV14.

tion which is consistent with previous works [19,38,39].

3.4 Effects of Initial Concentration of BV14 on Photodegradation

The initial dye concentration is a key factor to treat industrial pollutants. To investigate the effect of initial concentrations of BV14 on the photodegradation, several experiments were performed with different initial concentrations of BV14 varying from 3.0×10^{-5} M to 4.50×10^{-5} M and keeping suspension of A_3 nanocomposite constant as 0.1753 g/100 mL. Figure 9 shows that with the increase of initial concentration of BV14 photodegradation decreases. The results suggest that higher the initial concentration of BV14, lower the photodegradation of BV14. Similar results are also found in other studies for the photodegradation of other dyes [40–43]. With the higher concentration of BV14, the color of BV14 solution turns to be darker that causes reducing the penetration of light to the surface of the catalyst and lowering the number of energetic dye molecules that engender lower photodegradation of BV14.

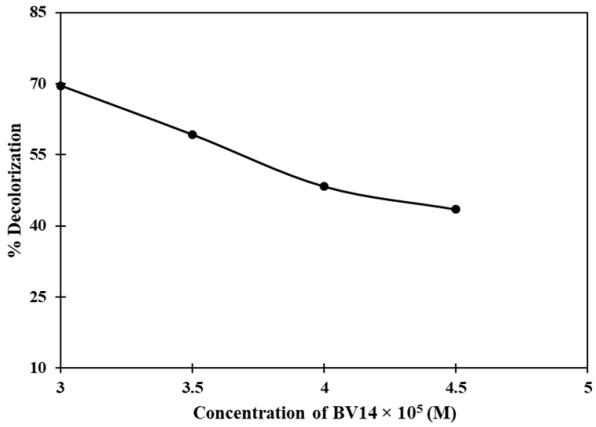

Figure 9. Effect of different initial concentrations of BV14 on the photodegradation.

3.5 Effects of Solution pH on the Photodegradation

The effect of pH was researched in the pH range 4.50 – 9.00 so that changes of phtodegradation of BV14 can be observed in acid, neutral and alkaline medium. In the Figure 10, it is shown that the percentage of photodegradation of BV14 is minimum at pH of 4.5 where the surface is positively charged, and dye BV14 is also positively charged in solution. Due to electrostatic repulsion, adsorption is the minimum triggering photodegradation minimum. As the pH increases, positive charge on the surface decreases, and adsorption will increase due to the increase of electrostatic force of attraction between surface and positively charged dye as a result photodegradation increases with the increase of pH [44,45]. It was also observed that photodegradation is the maximum at pH of 6.88 where the surface is almost neutral and beyond this pH, photodegradation starts to decrease. This is also aligned with other works [46]. With the increase of pH, the surface becomes negative, and it is expected that the adsorption of positively charged dye molecules should increase to negatively charged surface. However, the observation was not consistent with this assumption. This can be explained by the fact that in presence of light electron-hole separation occurs on the surface of the photocatalyst.

$$\text{Solid surface} + h\nu \rightleftharpoons h^+ + e^- \quad (1)$$

In basic media (pH 7 to 9), the surface is negative in nature and the negative electric

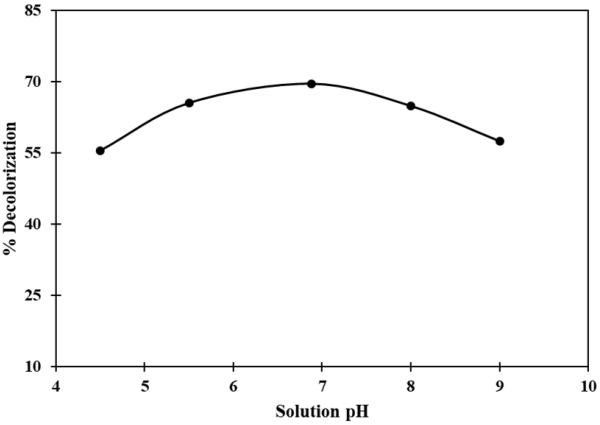

Figure 10. The effect of initial solution pH on degradation of BV14.

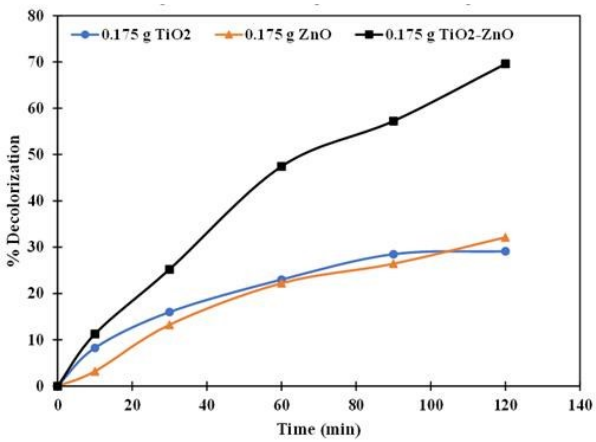

Figure 11. Comparison of photocatalytic property of TiO_2, ZnO, and TiO_2-ZnO composite.

field formed around nanocomposite particles is not favorable for the transfer of h^+ to the substrate. It can be predicted that reaction proceeds slowly through the formation of •OH radical.

$$TiO_2\text{-}ZnO\ (h^+) + H_2O \rightarrow \bullet OH + H^+ + TiO_2\text{-}ZnO \quad (2)$$

Then, the proton retained on the surface makes the positively charged dye molecules difficult to adsorb that slows down the adsorption. This process decreases with the increase of pH and finally, the adsorption and thereby photodegradation becomes minimum.

3.6 Comparison of Photocatalytic Property of ZnO, TiO_2, and TiO_2-ZnO Nanocomposite

Figure 11 demonstrates TiO_2, ZnO and TiO_2-ZnO mediated photodegradation of the BV14 dye. Among the three photocatalysts, the photodegradation is maximum for the prepared TiO_2-ZnO nanocomposite [20,47]. This attributes to a lower band gap energy of TiO_2-ZnO (3.09 eV) than that of solitary TiO_2 (3.20 eV) and ZnO (3.29 eV) oxide which conforms to the result of previous work [19].

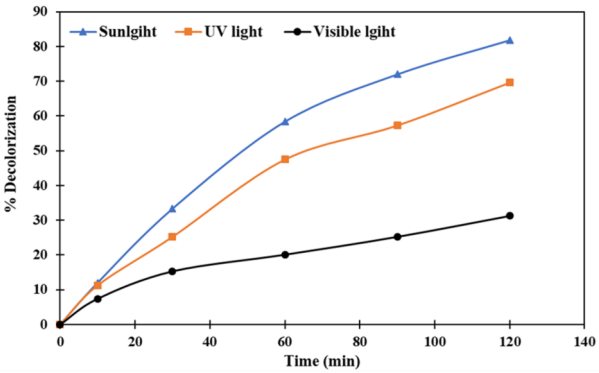

Figure 12. The effect of light sources on the photodegradation of BV14.

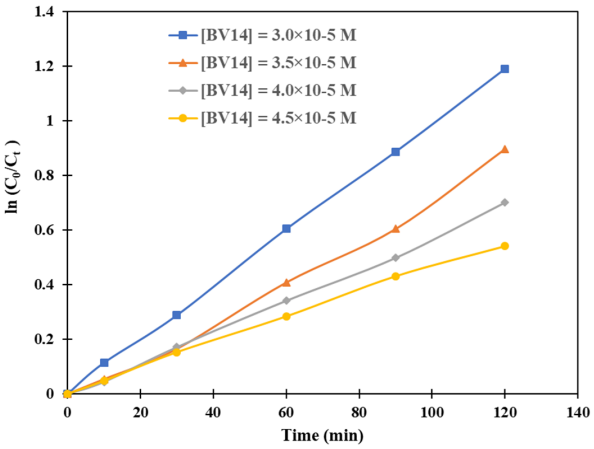

Figure 13. Kinetics study of photodegradation of BV14 for different initial concentrations.

3.7 Effects of Light Sources on the Photodegradation

In the Figure 12, the results are shown that percentages of degradation were 81.78%, 69.58%, and 31.24% under sunlight, UV light and visible light, respectively. It is reasonable to consider that the energy and intensity of the sunlight are higher than those of UV and visible light as a result, photodegradation is much higher when it is irradiated by the sunlight [20] instead of visible and UV light. Photodegradation increases with the increase in the intensity of light; this can be attributed to the fact that the number of photons striking per unit time per unit area of A_3 composite increases.

3.8 Kinetic Study of Photodegradation

According to the Langmuir-Hinshelwood equation [48]:

$$\frac{1}{k} = \frac{[BV14]_0}{k_c} + \left(\frac{1}{k_c}\right) K_{L-H} \quad (3)$$

Slope = $1/k_c$ = 18078097.225; k_c = 5.53×10^{-8} mol.L^{-1}.min^{-1}; Intercept = $(1/k_c)K_{L\text{-}H}$ = 109.357; $K_{L\text{-}H}$ = 1.7×10^8 L.mol^{-1}. According to the equation of the first order reaction [48]:

$$\ln\left(\frac{C_0}{C_t}\right) = k_c t \quad (4)$$

The photodegradation of BV14 follows pseudo 1st order kinetics with respect to the concentration of BV14 which was investigated by plotting a graph of $\ln(C_o/C_t)$ vs. irradiation time. The pseudo 1st order rate constants of photo-

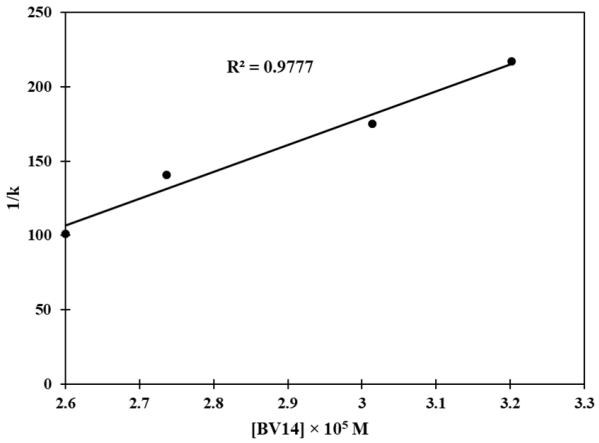

Figure 14. Evaluation of L-H model by plotting $1/k$ vs [BV14].

degradation of BV14 were found to be decreased with the increase of the concentration of BV14 as shown in the Figure 13. This result is aligned with other works [19]. This can be explained by the decreasing number of energetic sites on the photocatalyst surface due to covering the surface with BV14 molecules which is proportional to the initial concentration of BV14. Adsorption decreases due to decreasing vacant sites on the surface with the increase of BV14 concentration, this can be explained as decreasing photodegradation with the increase of substrate concentration [49]. A plot of $1/k$ vs $[BV14]_0$ gives a straight line that is shown in the Figure 14. So, it is evident that the photodegradation process follows Langmuir-Hinshelwood kinetics. From slope and intercept of this curve, the rate constant of surface reaction and the Langmuir-Hinshelwood adsorption constant were found to be 5.53×10^{-8} mol.L^{-1}.min^{-1} and 1.7×10^{8} L.mol^{-1}, respectively.

4. Conclusion

In present study, TiO_2-ZnO nanocomposite was successfully prepared and effectively applied to degrade industrial dye, BV14. The composite photocatalyst was characterized by the SEM, FTIR, EDX, and XRD. The peaks obtained from the XRD and EDX have established the presence of a composite photocatalyst of TiO_2-ZnO. With the help of SEM, the different particle sizes and shapes of TiO_2-ZnO nanocomposite were found by varying the temperatures during calcinations. Photodegradation of BV14 enhances with enhancement of light intensity. So, the maximum photodegradation was observed under sunlight and the minimum photodegradation was observed under visible light. It is found that the nature of light sources influences photodegradation of BV14. Nanocomposite A_3, prepared at high temperature (500 °C), degrades BV14 more effectively than nanocomposites A_1 and A_2 prepared at low temperature 300 °C and 400 °C, respectively. This abnormality was attributed to the larger surface area of rod-like shaped nanocomposite A_3. It is suggested that A_3 nanocomposite is an effective photocatalyst under sunlight irradiation. It is confirmed that photodegradation of BV14 follows pseudo first order kinetics. By all means, and with proven outcomes, this research has clearly demonstrated that TiO_2-ZnO acts as a better composite photocatalyst to decolorize BV14 under optimum experimental conditions such 3.0×10^{-5} M of BV14, 0.1753/100 g of composite, sunlight and neutral pH. In future studies, it is important to identify whether TiO_2-ZnO nanocomposite photocatalyst can be applied to degrade inorganic dyes.

Acknowledgments

The authors thank the Department of Chemistry, University of Dhaka, Dhaka. The authors also thank Centre for Advanced Research in Sciences (CARS), University of Dhaka, and Bangladesh University of Business and Technology (BUBT), Mirpur-2, Dhaka.

CRediT Author Statement

Md. Abdullah Bin Samad: Conceptualization, Methodology, Writing-Original draft preparation, Data curation. Dr. Emran Quayum: Supervision. Md. Amjad Hossain: Conceptualization, Methodology, Software, Editing. Dr. Tajmeri S.A. Islam: Visualization, Investigation, Validation. Mohammad Mahmudur Rahman Khan: Writing- Reviewing and Editing.

References

[1] Rabbi, A.M., Hasan, M.M., Akhter, A. (2016). Heavy metals content in inlet water, treated and untreated waste water of garments industries at Gazipur, Bangladesh. *Environmental Science An Indian Journal*, 12 (4), 133–136.

[2] Castillo, M., Alonso, M.C., Riu, J., Barceló, D. (1999). Identification of Polar, Ionic, and Highly Water Soluble Organic Pollutants in Untreated Industrial Wastewaters. *Environmental Science & Technology*, 33(8), 1300–1306. DOI: 10.1021/es981012b.

[3] Kabir, S.M., Hasan, M., Uddin, Z. (2019). Novel Approach to Dye Polyethylene Terephthalate (PET) Fabric in Supercritical Carbon Dioxide with Natural Curcuminoid Dyes. *Fibres and Textiles in Eastern Europe*, 27(3(135)), 65–70. DOI: 10.5604/01.3001.0013.0744.

[4] Hasan, M., Hossain, M.B., Reza, S. (2014). Application of Purified Curcumin as Natural Dye on Cotton and Polyester. *International Journal of Engineering*, 14 (05), 17–23.

[5] Sakthivel, S., Neppolian, B., Shankar, M.V., Arabindoo, B., Palanichamy, M., Murugesan, V. (2003). Solar photocatalytic degradation of azo dye: Comparison of photocatalytic efficiency of ZnO and TiO_2. *Solar Energy Materials and Solar Cells*, 77(1), 65–82. DOI: 10.1016/S0927-0248(02)00255-6.

[6] Modirshahla, N., Ali, M., Oskui, J., Reza, M. (2009). Investigation of the Efficiency of ZnO Photocatalyst in the Removal of p-Nitrophenol from Contaminated Water. *Iranian Journal of Chemistry and Chemical Engineering*, 28(1), 49–55. DOI: 10.30492/IJCCE.2009.6914.

[7] Carp, O., Huisman, C.L., Reller, A. (2004). Photoinduced reactivity of titanium dioxide. *Progress in Solid State Chemistry*, 32, 33–177. DOI: 10.1016/j.progsolidstchem.2004.08.001.

[8] Ahmad, N., Fitri, E. S., Wijaya, A., Amri, A., Mardiyanto, M., Royani, I., Lesbani, A. (2022). Catalytic Oxidative Desulfurization of Dibenzothiophene Utilizing Composite Based Zn/Al Layered Double Hydroxide. *Bulletin of Chemical Reaction Engineering & Catalysis*, 17(4), 733–742. DOI: 10.9767/bcrec.17.4.15335.733-742.

[9] Ahmad, N., Yuliasari, N., Arsyad, F., Royani, I., Mohadi, R., Lesbani, A. (2023). Catalytic oxidative desulfurization of dibenzothiophene by heterogeneous M2/Al-layered double hydroxide (M2+ = Zn, Mg, Ni) modified zinc oxide. *Iranian Journal of Catalysis*, 13, 35–45. DOI: 10.30495/ijc.2023.1972458.1973.

[10] Saeed, M., Ibrahim, M., Muneer, M., Akram, N., Usman, M., Maqbool, I., Adeel, M., Nisar, A. (2021). ZnO–TiO_2: Synthesis, Characterization and Evaluation of Photo Catalytic Activity towards Degradation of Methyl Orange. *Zeitschrift Für Physikalische Chemie*, 235(3), 225–237. DOI: 10.1515/zpch-2019-1536.

[11] Hossain, M.A., Samad, M.A.B., Khan, D.H., Ara, N.J., Islam, T.S.A. (2018). Study of ZnO-TiO_2 Composite Photocatalyst Mediated Photodegradation of Eosin Yellow. *IOSR Journal of Environmental Science, Toxicology and Food Technology*, 12(6), 58–67. DOI: 10.9790/2402-1206025867

[12] Wang, L., Fu, X., Han, Y., Chang, E., Wu, H., Wang, H., Li, K., Qi, X. (2013). Preparation, Characterization, and Photocatalytic Activity of TiO_2 /ZnO Nanocomposites. *Journal of Nanomaterials*, 2013, 321459. DOI: 10.1155/2013/321459.

[13] Talebi, S., Chaibakhsh, N., Moradi-Shoeili, Z. (2017). Application of nanoscale ZnS/TiO2 composite for optimized photocatalytic decolorization of a textile dye. *Journal of Applied Research and Technology*, 15(4), 378–385. DOI: 10.1016/j.jart.2017.03.007.

[14] Almhana, N., Naser, Z., Al-Najjar, S., Al-Sharify, Z., Nail, T. (2022). Photocatalytic Degradation of Textile Dye from Wastewater by using ZnS/TiO_2 Nanocomposites Material. *Egyptian Journal of Chemistry*, 65(131), 481–488. DOI: 10.21608/ejchem.2022.125852.5588.

[15] Dhatshanamurthi, P., Subash, B., Krishnakumar, B., Shanthi, M. (2014). Highly active ZnS loaded TiO_2 photocatalyst for mineralization of phenol red sodium salt under UV-A light. *Indian Journal of Chemistry*, 53, 820–823.

[16] Marcì, G., Augugliaro, V., López-Muñoz, M. J., Martín, C., Palmisano, L., Rives, V., Schiavello, M., Tilley, R.J.D., Venezia, A.M. (2001). Preparation Characterization and Photocatalytic Activity of Polycrystalline ZnO/TiO_2 Systems. 2. Surface, Bulk Characterization, and 4-Nitrophenol Photodegradation in Liquid−Solid Regime. *The Journal of Physical Chemistry B*, 105 (5), 1033–1040. DOI: 10.1021/jp003173j.

[17] Siuleiman, S.A., Raichev, D.V., Bojinova, A.S., Dimitrov, D.T., Papazova, K.I. (2013). Nanosized composite ZnO/TiO_2 thin films for photocatalytic applications. *Bulgarian Chemical Communications*, 45(4), 649–654.

[18] Shalaby, A., Bachvarova-Nedelcheva, A., Dimitriev, Y., Iordanova, R., Stoyanova, A., & Sredkova, M. (2011). Antibacterial Properties of $ZnTiO_3$ Prepared by Sol-Gel Method. *Journal of Optoelectronics and Biomedical Materials,* 3(2), 39–44.

[19] Habib, M.A., Shahadat, M.T., Bahadur, N.M., Ismail, I.M.I., Mahmood, A.J. (2013). Synthesis and characterization of ZnO-TiO_2 nanocomposites and their application as photocatalysts. *International Nano Letters*, 3(1), 5. DOI: 10.1186/2228-5326-3-5.

[20] Jiang, Y., Sun, Y., Liu, H., Zhu, F., Yin, H. (2008). Solar photocatalytic decolorization of C.I. Basic Blue 41 in an aqueous suspension of TiO_2–ZnO. *Dyes and Pigments*, 78(1), 77–83. DOI: 10.1016/j.dyepig.2007.10.009.

[21] Messaoudi, Z.A., Lahcene, D., Benaissa, T., Messaoudi, M., Zahraoui, B., Belhachemi, M., ChoukchouBraham, A. (2022). Adsorption and Photocatalytic Degradation of Crystal Violet Dye under Sunlight Irradiation Using Natural and Modified Clays by Zinc Oxide. *Chemical Methodologies*, 6(9), 661–676. DOI: 10.22034/chemm.2022.340376.1507.

[22] Danish, M.S.S., Estrella, L.L., Alemaida, I.M.A., Lisin, A., Moiseev, N., Ahmadi, M., Nazari, M., Wali, M., Zaheb, H., Senjyu, T. (2021). Photocatalytic Applications of Metal Oxides for Sustainable Environmental Remediation. *Metals*, 11(1), 80. DOI: 10.3390/met11010080.

[23] Bozkurt Çırak, B., Caglar, B., Kılınç, T., Morkoç Karadeniz, S., Erdoğan, Y., Kılıç, S., Kahveci, E., Ercan Ekinci, A., Çırak, Ç. (2019). Synthesis and characterization of ZnO nanorice decorated TiO_2 nanotubes for enhanced photocatalytic activity. *Materials Research Bulletin*, 109, 160–167. DOI: 10.1016/j.materresbull.2018.09.039.

[24] Mohamed, S.K., Hegazy, Sh.H., Abdelwahab, N.A., Ramadan, A.M. (2018). Coupled adsorption-photocatalytic degradation of crystal violet under sunlight using chemically synthesized grafted sodium alginate/ZnO/graphene oxide composite. *International Journal of Biological Macromolecules*, 108, 1185–1198. DPI: 10.1016/j.ijbiomac.2017.11.028.

[25] Pragathiswaran, C., Smitha, C., Mahin Abbubakkar, B., Govindhan, P., Anantha Krishnan, N. (2021). Synthesis and characterization of TiO_2/ZnO–Ag nanocomposite for photocatalytic degradation of dyes and antimicrobial activity. *Materials Today: Proceedings*, 45, 3357–3364. DOI: 10.1016/j.matpr.2020.12.664.

[26] Ismail, M., Akhtar, K., Khan, M.I., Kamal, T., Khan, M.A., Asiri, A.M., Seo, J., Khan, S.B. (2019). Pollution, Toxicity and Carcinogenicity of Organic Dyes and their Catalytic Bio-Remediation. *Current Pharmaceutical Design*, 25(34), 3645–3663. DOI: 10.2174/1381612825666191021142026.

[27] Bao, H.V., Dat, N.M., Giang, N.T.H., Thinh, D.B., Tai, L.T., Trinh, D.N., Hai, N.D., Khoa, N.A.D., Huong, L.M., Nam, H.M., Phong, M.T., Hieu, N.H. (2021). Behavior of ZnO-doped TiO_2/rGO nanocomposite for water treatment enhancement. *Surfaces and Interfaces*, 23, 100950. DOI: 10.1016/j.surfin.2021.100950.

[28] Hussain, S.M., Hussain, T., Faryad, M., Ali, Q., Ali, S., Rizwan, M., Hussain, A.I., Ray, M.B., Chatha, S.A.S. (2020). Emerging Aspects of Photo-catalysts (TiO_2 & ZnO) Doped Zeolites and Advanced Oxidation Processes for Degradation of Azo Dyes: A Review. *Current Analytical Chemistry*, 17(1), 82–97. DOI: 10.2174/1573411016999200711143225.

[29] Jaramillo-Fierro, X., González, S., Jaramillo, H.A., Medina, F. (2020). Synthesis of the $ZnTiO_3$/TiO_2 Nanocomposite Supported in Ecuadorian Clays for the Adsorption and Photocatalytic Removal of Methylene Blue Dye. *Nanomaterials*, 10 (9), 1891. DOI: 10.3390/nano10091891.

[30] Samsuri, S.A.M., Rahman, M.Y.A., Umar, A.A. (2017). Comparative study of the properties of TiO_2 nanoflower and TiO_2-ZnO composite nanoflower and their application in dye-sensitized solar cells. *Ionics*, 23(7), 1897–1902. DOI: 10.1007/s11581-017-2010-4.

[31] Zuas, O., Hamim, N. (2013). Synthesis, Characterization and Properties of CeO_2-doped TiO_2 Composite Nanocrystals. *Materials Science*, 19(4), 443–447. DOI: 10.5755/j01.ms.19.4.2732.

[32] Gao, Y., Masuda, Y., Koumoto, K. (2004). Light-Excited Superhydrophilicity of Amorphous TiO_2 Thin Films Deposited in an Aqueous Peroxotitanate Solution. *Langmuir*, 20(8), 3188–3194. DOI: 10.1021/la0303207.

[33] Hamza, M.A., Saiof, F.N., Al-ithawi, A.S., Ameen, M.A., Yaseen, H.M. (2013). Prepared of Nd:TiO_2 Nano Particles Powder as IR Filter via Sol-Gel. *Advances in Materials Physics and Chemistry*, 03(02), 174–177. DOI: 10.4236/ampc.2013.32024.

[34] Chen, C., Yu, B., Liu, P., Liu, J., Wang, L. (2011). Investigation of nano-sized ZnO particles fabricated by various synthesis routes. *Journal of Ceramic Processing Research*, 12(4), 420–425.

[35] Thamaphat, K., Limsuwan, P., Ngotawornchai, B. (2008). Phase Characterization of TiO_2 Powder by XRD and TEM. *Agriculture and Natural Resources*, 42(5), 357–361.

[36] Kim, D.S., Park, Y.S. (2006). Photocatalytic decolorization of rhodamine B by immobilized TiO_2 onto silicone sealant. *Chemical Engineering Journal*, 116(2), 133–137. DOI: 10.1016/j.cej.2005.10.013.

[37] Daneshvar, N., Aber, S., Seyeddorraji, M., Khataee, A., Rasoulifard, M. (2007). Photocatalytic degradation of the insecticide diazinon in the presence of prepared nanocrystalline ZnO powders under irradiation of UV-C light. *Separation and Purification Technology*, 58(1), 91–98. DOI: 10.1016/j.seppur.2007.07.016.

[38] Behnajady, M., Modirshahla, N., Hamzavi, R. (2006). Kinetic study on photocatalytic degradation of C.I. Acid Yellow 23 by ZnO photocatalyst. *Journal of Hazardous Materials*, 133(1–3), 226–232. DOI: 10.1016/j.jhazmat.2005.10.022.

[39] Muruganandham, M., Sobana, N., Swaminathan, M. (2006). Solar assisted photocatalytic and photochemical degradation of Reactive Black 5. *Journal of Hazardous Materials*, 137(3), 1371–1376. DOI: 10.1016/j.jhazmat.2006.03.030.

[40] Akyol, A., Yatmaz, H.C., Bayramoglu, M. (2004). Photocatalytic decolorization of Remazol Red RR in aqueous ZnO suspensions. *Applied Catalysis B: Environmental*, 54(1), 19–24. DOI: 10.1016/j.apcatb.2004.05.021.

[41] Barka, N., Qourzal, S., Assabbane, A., Nounah, A., Ait-Ichou, Y. (2010). Photocatalytic degradation of an azo reactive dye, Reactive Yellow 84, in water using an industrial titanium dioxide coated media. *Arabian Journal of Chemistry*, 3(4), 279–283. DOI: 10.1016/j.arabjc.2010.06.016.

[42] Muruganandham, M., Swaminathan, M. (2006). Photocatalytic decolourisation and degradation of Reactive Orange 4 by TiO-UV process. *Dyes and Pigments*, 68(2–3), 133–142. DOI: 10.1016/j.dyepig.2005.01.004.

[43] Sahoo, C., Gupta, A.K., Pal, A. (2005). Photocatalytic degradation of Methyl Red dye in aqueous solutions under UV irradiation using Ag^+ doped TiO_2. *Desalination*, 181(1–3), 91–100. DOI: 10.1016/j.desal.2005.02.014.

[44] Hu, C., Tang, Y., Yu, J.C., Wong, P.K. (2003). Photocatalytic degradation of cationic blue X-GRL adsorbed on TiO_2/SiO_2 photocatalyst. *Applied Catalysis B: Environmental*, 40(2), 131–140. DOI: 10.1016/S0926-3373(02)00147-9.

[45] Shimizu, N., Ogino, C., Dadjour, M.F., Murata, T. (2007). Sonocatalytic degradation of methylene blue with TiO_2 pellets in water. *Ultrasonics Sonochemistry*, 14(2), 184–190. DOI: 10.1016/j.ultsonch.2006.04.002.

[46] Chen, C.C. (2007). Degradation pathways of ethyl violet by photocatalytic reaction with ZnO dispersions. *Journal of Molecular Catalysis A: Chemical*, 264(1–2), 82–92. DOI: 10.1016/j.molcata.2006.09.013.

[47] Siwińska-Stefańska, K., Kubiak, A., Piasecki, A., Goscianska, J., Nowaczyk, G., Jurga, S., Jesionowski, T. (2018). TiO_2-ZnO Binary Oxide Systems: Comprehensive Characterization and Tests of Photocatalytic Activity. *Materials*, 11(5), 841. DOI: 10.3390/ma11050841.

[48] Khan, M.S., García, M.F., Javed, M., Kubacka, A., Caudillo-Flores, U., Halim, S.A., Khan, A., Al-Harrasi, A., Riaz, N. (2021). Synthesis, Characterization, and Photocatalytic, Bactericidal, and Molecular Docking Analysis of Cu–Fe/TiO_2 Photocatalysts: Influence of Metallic Impurities and Calcination Temperature on Charge Recombination. *ACS Omega*, 6(40), 26108–26118. DOI: 10.1021/acsomega.1c03102.

[49] Daneshvar, N., Aber, S., Dorraji, M.S.S., Khataee, A.R., Rasoulifard, M.H. (2007). Preparation and Investigation of Photocatalytic Properties of ZnO Nanocrystals: Effect of Operational Parameters and Kinetic Study. *International Journal of Nuclear and Quantum Engineering*, 1(5), 62–67.